


## IRT DOCUMENTATION PAGE

1a. <b>AD-A236 101</b> 			1b. RESTRICTIVE MARKINGS None		
2a.			3. DISTRIBUTION / AVAILABILITY OF REPORT Approved for public release and sale. Distribution unlimited.		
2b. DECLASSIFICATION / DOWNGRADING SCHEDULE					
4. PERFORMING ORGANIZATION REPORT NUMBER(S) ONR Technical Report No. 27			5. MONITORING ORGANIZATION REPORT NUMBER(S)		
6a. NAME OF PERFORMING ORGANIZATION University of Utah		6b. OFFICE SYMBOL (If applicable)		7a. NAME OF MONITORING ORGANIZATION	
6c. ADDRESS (City, State, and ZIP Code) Department of Chemistry Henry Eyring Building Salt Lake City, UT 84112		7b. ADDRESS (City, State, and ZIP Code)			
8a. NAME OF FUNDING / SPONSORING ORGANIZATION Office of Naval Research		8b. OFFICE SYMBOL (If applicable)		9. PROCUREMENT INSTRUMENT IDENTIFICATION NUMBER N00014-89-J-1412	
8c. ADDRESS (City, State, and ZIP Code) Chemistry Program, Code 1113 800 N. Quincy Street Arlington, VA 22217		10. SOURCE OF FUNDING NUMBERS			
		PROGRAM ELEMENT NO		PROJECT NO	TASK NO
					WORK UNIT ACCESSION NO
11. TITLE (Include Security Classification) Quantitative Investigation of Charge-Trapping Effects on Raman Spectra Acquired Using Charge-Coupled Device (CCD) Detectors					
12. PERSONAL AUTHOR(S) W. B. Lacy, K. L. Rowlen, and J. M. Harris					
13a. TYPE OF REPORT Technical		13b. TIME COVERED FROM 6/90 TO 5/91		14. DATE OF REPORT (Year, Month, Day) May 22, 1991	
15. PAGE COUNT 23					
16. SUPPLEMENTARY NOTATION					
17. COSATI CODES			18. SUBJECT TERMS (Continue on reverse if necessary and identify by block number)		
FIELD	GROUP	SUB-GROUP	Raman spectroscopy; Charge-coupled device (CCD) detectors; Spectroscopic artifacts.		
19. ABSTRACT (Continue on reverse if necessary and identify by block number)  Attached.					
20. DISTRIBUTION / AVAILABILITY OF ABSTRACT <input checked="" type="checkbox"/> UNCLASSIFIED/UNLIMITED <input type="checkbox"/> SAME AS RPT <input type="checkbox"/> DTIC USERS			21. ABSTRACT SECURITY CLASSIFICATION Unclassified		
22a. NAME OF RESPONSIBLE INDIVIDUAL Joel M. Harris			22b. TELEPHONE (Include Area Code) (801)581-3585		22c. OFFICE SYMBOL

**DTIC**  
**ELECTE**  
**MAY 30 1991**  
**S E D**



OFFICE OF NAVAL RESEARCH

Grant No: N00014-89-J-1412

R&T Code 413a005---03

Technical Report No. 27

Accession For	
NTIS GRA&I	<input checked="" type="checkbox"/>
DTIC TAB	<input type="checkbox"/>
Unannounced	<input type="checkbox"/>
Justification	
By	
Distribution/	
Availability Codes	
Dist	Avail and/or Special
A-1	

Quantitative Investigation of Charge-Trapping Effects on Raman Spectra

Acquired Using Charge-Coupled Device (CCD) Detectors

Prepared for publication in Applied Spectroscopy

by

W. B. Lacy, K. L. Rowlen, and J. M. Harris

Department of Chemistry  
University of Utah  
Salt Lake City, UT 84112

May 22, 1991

**91-00659**



Reproduction in whole, or in part, is permitted for  
any purpose of the United States Government

\* This document has been approved for public release and sale;  
its distribution is unlimited.

**91 5 29 016**

QUANTITATIVE INVESTIGATION OF CHARGE-TRAPPING EFFECTS ON RAMAN SPECTRA  
ACQUIRED USING CHARGE-COUPLED DEVICE (CCD) DETECTORS

W. B. Lacy, K. L. Rowlen<sup>†</sup>, and J. M. Harris<sup>\*</sup>  
Department of Chemistry  
University of Utah  
Salt Lake City, UT 84112

ABSTRACT

Changes in spectral band parameters (width, center frequency, intensity) which arise from charge-trapping artifacts in the Thomson TH 7882 charge-coupled device (CCD) detector are reported. These parameters are measured for a Raman scattering band of carbon tetrachloride with respect to CCD geometry (parallel versus serial binning), in the presence and absence of preflash, versus changes in integration time (variation in detected light level). The dependence of the spectral parameters on detector temperature was also measured. The degree of charge trapping and the charge transfer efficiency were estimated from the change in peak width and intensity versus integration time, respectively, and were found to vary with detector temperature according to an Arrhenius relationship for the serial-binning geometry; from these results, the energy barriers to charge trapping and loss in the serial register were estimated. Practical guidelines for acquisition of binned spectra with this detector are suggested.

<sup>†</sup> Present Address: Department of Chemistry, University of Colorado, Boulder, CO 80309-0215

<sup>\*</sup> Author to whom correspondence should be addressed.

Index Headings: Charge-coupled device (CCD); Spectroscopic Instrumentation; Raman Spectroscopy.

## INTRODUCTION

The application of charge-coupled device (CCD) detectors in analytical spectroscopy has increased dramatically in recent years (1-5). The CCD, a two-dimensional silicon-metal oxide array, is nearly ideal for a variety of spectroscopic techniques, especially those requiring detection at low light levels. Charge-coupled device detectors have a number of characteristic advantages over other multichannel detectors, including high quantum efficiency in the visible and near-IR, excellent charge transfer efficiency, low read noise and dark current, wide dynamic range, and image plane stability. The characteristics and operation of CCD detectors have been presented in several recent reviews (2,6-7).

Utilization of the CCD as a spectroscopy detector is based on collecting and storing photon-induced charge on a continuous silicon substrate divided into individual elements (pixels) by a series of electrodes which are used to manipulate the charge. Exposure of this two-dimensional imaging area, called the parallel register, to light leads to charge separation at the n-p junction, and an image of charge accumulates localized by potential wells established by electrodes on the detector surface. This charge image can be propagated row-by-row across the CCD by a series of potentials applied to the electrodes. The charge is then be transferred to a second, one-dimensional array, called the serial register. During readout, the serial register is emptied into the output node of the device and re-filled with the next row of charge. This process continues until the entire array is emptied of charge. Charge-coupled device detectors have an additional capability which greatly benefits spectroscopic applications, that of on-chip signal averaging or binning (8,9). Binning is the process by which charge on adjacent pixels is combined either by

row (parallel) or by column (serial) prior to digitization.

Transfer of charge across the parallel register exhibits finite charge transfer efficiency (10) along with charge trapping arising from a threshold charging level required to observe efficient charge transfer (11); while the former artifact influences the detector sensitivity, the latter artifact can influence both detector linearity and charge spreading distribution. Pemberton and co-workers (12) have recently reported that spectra from a Thomson TH 7882 CCD binned in the serial register are distorted due to charge trapping; they reported that the distortion is greater at smaller incident intensity and integration times and that the effect was minimal when binning in the parallel orientation. In the study conducted by Pemberton et al., no preflash was employed. A prior exposure of the chip to radiation of uniform intensity can be used to partially fill the charge wells; this preflash is typically achieved by using a ring of light emitting diodes surrounding the chip (9). While a preflash is known to reduce charge-trapping effects, its use in low background, high sensitivity measurements can degrade detection limits due to the increased shot noise from the higher background of photoelectrons. In addition to the influence of preflash on the charge trap artifact, there are reports that the operating temperature affects the charge-trapping characteristics of the Thomson TH 7882 CCD (13). Unfortunately, there has been no report of a quantitative investigation of charge-trapping effects in CCD detected spectra and their dependence on preflash conditions, integrated intensity, and detector temperature.

Detector-induced bandshape distortions are of great concern to interpretation of spectroscopic data, where the results often depend on subtle changes in bandshape parameters. Instrumental distortions which depend on experimental

conditions are easily misinterpreted. While the problem of spectral distortions arising from charge trapping in CCD's has been identified, a quantitative investigation of its effect on spectroscopic bandshapes is needed. The goal of this study, therefore, is to report changes in spectral band parameters (width, center frequency, intensity) which arise from charge transfer artifacts. These parameters were measured for a Raman scattering band of carbon tetrachloride with respect to CCD geometry (parallel versus serial binning), in the presence and absence of preflash, versus changes in integration time (variation in detected light level). The dependence of the spectral parameters on detector temperature was also measured for the serial- and parallel-binning geometries. The degree of charge trapping and the charge transfer efficiency were estimated from the change in peak width and intensity versus integration time, respectively, and were found to vary with detector temperature according to an Arrhenius relationship in the serial-binning geometry; from these results, the energy barriers to charge trapping and loss in the serial register were estimated. Practical guidelines for acquisition of binned spectra with this detector are suggested.

## EXPERIMENTAL

The 514.5 nm line from an argon ion laser (Lexel, Model 95) was used for sample excitation. Incoherent plasma lines from the laser were eliminated by a combination of two Pellin Brocha prisms (Optics for Research, ABDU-20) and a variable aperture. The 90 mW beam was focused with a plano-convex lens ( $f=100.00$  mm) to an approximately 50  $\mu\text{m}$  spot size at the sample cell which was a borosilicate glass capillary (1 mm i.d., Kimax). Scattered light from the sample cell was collected and collimated at  $90^\circ$  from excitation by an F/1.8

camera lens (Canon, 50 mm), and focused by a plano-convex lens (F/3.9,  $f=100.00$  mm) into the entrance slit of the monochromator (0.5 m, Spex 1870). The slit width was 60  $\mu\text{m}$  for all spectra. A Raman notch filter (Omega, 514.5 nm cutoff, 7.2 nm band width at 10% T) was placed between the collection and focusing lenses and transmitted less than a  $10^{-5}$  fraction of the Rayleigh scatter at 514.5 nm. Some experiments required combinations of neutral density filters to be placed between the sample and monochromator to assure that the peak of interest ( $214\text{ cm}^{-1}$  peak of  $\text{CCl}_4$ ) remained on scale. These combinations were not varied within any set of measurements. Carbon tetrachloride (Burdick & Jackson, spectroscopic grade) was acquired from Baxter and used as received.

A 1200 groove/mm grating dispersed the scattered radiation across a Thomson TH 7882 charge-coupled device (Series 200, Photometrics, Ltd., Tuscon, AZ). The format of the silicon-metal oxide chip is 576 rows by 384 columns, providing 221,184 pixels (1 pixel =  $23\text{ }\mu\text{m} \times 23\text{ }\mu\text{m}$ ) for detection. With the long axis oriented parallel to the direction of wavelength dispersion and the short axis along the slit axis, a Raman spectral range of approximately  $520\text{ cm}^{-1}$  could be detected; with the short axis oriented along to the direction of wavelength dispersion, the spectral coverage was reduced to approximately  $335\text{ cm}^{-1}$ . Throughout this study, the geometry in which the axis of wavelength dispersion is along the 576 rows of the CCD is designated as the serial-binning geometry, and the orientation in which the axis of wavelength dispersion is along the 384 columns of the CCD is termed the parallel-binning geometry (See Figure 1). All spectra were acquired with the preamplifier gain of the CCD set at its most sensitive value (corresponding to a signal of 21.2 photoelectrons per ADU and readout noise of 6 photoelectrons). For all spectra, including those acquired in the parallel-binning orientation, 383 pixels were binned

along the vertical axis of the chip to improve the signal-to-noise ratio. The temperature of the CCD chip was controlled to within  $\pm 0.1^\circ\text{C}$  by a thermoelectric cooler, heat exchanged to liquid nitrogen. For experiments which involved the preflash, a value of 70 for the preflash intensity parameter was used.

The camera controller unit (Photometrics Ltd., CC-200) was interfaced via an IEEE-488 bus to a very slow Apple Macintosh IIcx through an interface board (GPIB-2, National Instruments). Data were processed off-line, on an Arche 286 (IBM-AT compatible clone). Peak modeling was accomplished by using the baseline correction and curve fit (Chi-square minimization) routines in SpectraCalc (Galactic Industries). The effect of charge trapping on peak parameters was studied by fitting a single Lorentzian function to the  $214\text{ cm}^{-1}$  band of  $\text{CCl}_4$ ; this band was chosen for this study because the Raman spectrum in the gas phase (14) indicates that the band is well isolated from other bands in the spectrum. The errors associated with fitting a measured spectra to the Lorentzian band shape were negligible; starting the non-linear least squares fit from different initial values led to identical results. The reproducibility from one observation of a spectrum to the next were limited by shot noise; band center and width estimates varied less than  $\pm 0.05$  pixels.

## RESULTS AND DISCUSSION

Effect of Integrated Intensity on Charge-trapping Artifacts. The most obvious effect of charge trapping in CCD detected spectra are changes in measured peak width which depend on exposure. To illustrate this artifact, the  $214\text{ cm}^{-1}$  Raman scattering band of carbon tetrachloride was measured without detector preflash at various integration times with the CCD in a serial-binning configuration, and the results are plotted in Figure 2(a). The peak width



varies significantly with integration time for this geometry, as shown in Figure 3, especially without preflash. For the serial-binning orientation, when a preflash is used to provide electrons to partially fill the charge wells, the change in band width is minimal (less than one pixel) over the range of integration times. Without preflash, however, there is a dramatic increase (11-12 pixels) in the peak width, as seen in Figures 2(a) and 3, for exposures less than 10 sec or 8800 photoelectrons at the peak (rate of detected photoelectrons at the band center is  $\sim 880 \text{ sec}^{-1}$ ). A similar study of the parallel-binning orientation is presented in Figures 2(b) and 4. In the parallel geometry, the band width change is smaller and more symmetric. When a preflash is used, the change is less than one pixel. Without a preflash, however, a decrease in band width is observed when exposures are less than 7 sec or 6200 photoelectrons at the peak; the magnitude of the change in band width is 6-7 pixels or about 50% smaller than the distortions in the serial-binning orientation.

Since the above threshold values for the number of photoelectrons required to avoid distortions in band width are the result of binning charge along the slit axis, these values can be specified in terms of the number of photoelectrons per charge well by dividing by the number of illuminated pixels. The inner diameter of the capillary sample cell and magnification of the collection optics results in a sample image which is 2.2 mm at the detector, corresponding to 94 pixels. The thresholds for detected charge which avoid significant distortions in band width are, therefore,  $\sim 94 \text{ p.e.'s/pixel}$  for the case of serial binning and  $\sim 66 \text{ p.e.'s/pixel}$  for parallel binning. These values are smaller by a factor of  $\sim 5$  compared to the threshold coefficient specified previously in a study of the transfer efficiency of this detector (11); the

smaller values likely arise from the reduced impact of charge trapping in the serial register due to binning. The greater reduction in the threshold charge for minimal distortion is expected for parallel binning since the charge transferred in the serial register is the accumulated spectrum of the entire sample (see below).

As observed in Figures 2 - 4, with increasing light exposure, the band width increases to a stable value for the parallel-binning geometry and decreases to a stable value for the serial-binning geometry. This behavior can be explained in terms of how charges are summed and moved across the parallel and serial registers (see Figure 1). In the serial-binning geometry, only one row at a time is transferred across the parallel register to the serial register for binning. As a result, the 576 rows experience charge trapping as they are moved laterally across the parallel register. In the serial geometry at low light levels, no individual row has sufficient charge to overcome the minimum charge required for efficient charge transfer. Consider the impact on the Lorentzian lineshape obtained by binning in the serial geometry. As the leading edge of the Lorentzian is transferred across the parallel register, charge is lost upon each transfer and therefore not included in the intensity measurement because the charge traps are not yet full. As the trailing edge of the Lorentzian is transferred across the parallel register, the potential wells have acquired been exposed to sufficient charge from the peak of the band to allow efficient transfer, and there is no subsequent loss of charge. The result is a shortening of the leading edge and a broadening of the trailing edge which produces asymmetric band broadening. At longer integration times, when more charge is present, the charge traps fill earlier during the image transfer process and the distortion is minimized. In the parallel-binning

geometry, the charge contents of the rows of the parallel register are summed together in the serial register, which quickly accumulates sufficient charge to overcome charge trapping in subsequent serial readout of the spectrum. Charge is still lost as the spectral image is transferred in the parallel register and accumulated in the serial register, but since the total charge is contained in serial register, charge trapping in the serial transfer steps is eliminated. With sufficiently weak exposures (less than 7 sec. for our conditions), the effect of charge trapping in the parallel register is to reduce the width of the peak, as the less intense wings of the Lorentzian are partially lost to charge trapping while intense band center is transferred with a smaller loss.

Besides changes in band width, peak asymmetry can be introduced by charge trapping in the serial-binning orientation as described above. This is apparent in the variation of the observed band center with exposure as plotted in Figure 5. When a preflash is used, there is only a slight change in the band center as the integration time is reduced. A similarly well-behaved response is observed for the parallel-binning orientation independent of whether a preflash is used (see Figure 2(b)). A significant deviation from this behavior is observed in the serial geometry when a preflash is not supplied. Along with the increase in band width described above, there is a large change in the center frequency (11-12 pixels) for the serial geometry at integration times shorter than 30 seconds as shown in Figure 5.

Temperature-Dependence of Charge Trapping. To further characterize the charge-trapping artifact, the dependence of observed peak widths were monitored as a function of the CCD temperature, both with and without a preflash. Spectra were acquired using both chip orientations, at integration times short enough to observe charge trapping, while CCD temperature was varied from -115°C

to  $-85^{\circ}\text{C}$  in steps of  $10^{\circ}\text{C}$ . The  $214\text{ cm}^{-1}$  Raman scattering band of carbon tetrachloride was fit with to a Lorentzian function as above. As expected, with the CCD oriented in the parallel geometry and used without preflash, the band width was affected by charge trapping at the shortest integration times, but the distortion was independent of temperature over the range tested. Similarly, when using the serial geometry with a preflash, the small change in band width at the shortest exposure times increased from 0.2 pixels to 0.3 pixels when the detector temperature was raised from  $-115^{\circ}\text{C}$  to  $-85^{\circ}\text{C}$ . When the serial geometry was employed without preflash, however, the significant band broadening observed at the lowest integration time was found to be sensitive to temperature. At a 3 second integration time, the observed peak width increased by a full pixel at the highest temperature, as shown in Figure 6.

In an attempt to quantify this effect, the log of band width observed at a 3 sec exposure was plotted versus  $1/T$ ; the resulting plot was linear ( $r^2 = 0.94$ ) indicating that the temperature dependence of charge trapping appears to follow an Arrhenius relationship. While one might anticipate that electrons might escape a charge trap at higher temperatures and reduce the magnitude of the artifact, the greater band width at higher temperatures indicates that there is a small energy barrier to charge trapping in this range of  $kT$ . The magnitude of this barrier to charge trapping was estimated from the slope of the Arrhenius plot, and found to be  $5 \pm 2\text{ mV}$ . At the lower temperatures, the electrons have less thermal energy to overcome the barrier and the effects of charge trapping are reduced. At longer integration times (20-40 seconds) or in the presence of a preflash, where trapping has negligible effect on charge transfer, peak widths were found to exhibit no temperature dependence.

The choice of parallel versus serial binning not only affects the degree to which charge trapping distorts the shape of spectral bands as described above, it can also lead to differences in the efficiency of charge transfer on the parallel register affecting sensitivity. To study the CCD charge transfer efficiency, spectra were acquired at long integration times (20-40 seconds) so that charge trapping would not interfere in the band shape parameters. For parallel binning, both with and without the use of a preflash, the peak intensities and areas increase linearly with exposure with a sensitivity that was independent of temperature; the slope of the temperature dependence is indistinguishable from zero (see Figure 7). With the serial-binning geometry, however, the dependence of the intensity on integration time is also linear, but the sensitivity is smaller and depends on detector temperature. At the highest temperature ( $-85^{\circ}\text{C}$ ), the sensitivity of the detector in the serial-binning geometry is degraded by 15% compared to parallel binning, but converges to the same sensitivity as parallel binning at a sufficiently low temperature ( $-115^{\circ}\text{C}$ ). The slopes of the Arrhenius plots of Figure 7 for the serial-binning direction are independent of preflash conditions; the energy barrier to charge loss inferred from these results is  $13 \pm 2$  mV, or 2.5 times larger than the apparent barrier to charge trapping estimated from the increase in peak width. Based on this discrepancy, these two phenomena likely arise from different sources although both temperature-dependent charge transfer artifacts were found to arise in the serial-binning process. Since the clock rate for charge transfer in the serial register is 8-times faster than for the parallel register, any thermally-activated kinetic barriers to trapping or loss of charge during the transfer process are more likely to be observed in the serial register.

Conclusions. Regardless of the physical origins of charge trapping and losses in the Thomson TH 7882 CCD, practical guidelines for acquisition of binned spectra with this detector can be recommended from these results. As Pemberton and coworkers (12) previously concluded, significant distortion of spectral bands is observed when spectra are acquired in the serial-binning geometry without a preflash. The present results show that a preflash eliminates most of the distortion, but a sensitivity loss is observed for binning in this orientation when the detector temperature is greater than  $-115^{\circ}\text{C}$ . Operating the detector in the serial geometry at lower temperatures was found not only to eliminate the sensitivity loss but also to decrease the magnitude of the band distortion due to charge trapping.

The parallel-binning orientation avoids some, but not all, of the band distortion due to charge trapping. The band distortion was more symmetric, smaller in magnitude, and confined to lower exposure conditions than the serial-binning artifact; distortion could again be eliminated by use of a preflash. While the parallel-binning detector orientation suffers from a 35% smaller spectral range than the serial-binning orientation due to the smaller number of pixels along the wavelength axis, it provides a significant improvement in readout rate since the spectrum is co-added in parallel, greatly reducing the number of charge transfer steps. Despite the 8-fold faster clock rate for the serial register in our present detector, the time required to bin and readout a spectrum in the serial orientation is a sluggish 450 ms; while for the parallel orientation, the required time for binning and readout is only 10 ms.

#### ACKNOWLEDGEMENT

This work was supported in part by a grant from the Office of Naval Research.

## REFERENCES

1. J. V. Sweedler, R. B. Bilhorn, P. M. Epperson, G. R. Sims, and M. B. Denton, *Anal. Chem.* **60**, 282A (1988).
2. P. M. Epperson, J. V. Sweedler, R. B. Bilhorn, G. R. Sims, and M. B. Denton, *Anal. Chem.* **60**, 327A (1988).
3. A. Campion and S. S. Perry, *Laser Focus World*. August, 113 (1990).
4. R. B. Bilhorn, J. V. Sweedler, P. M. Epperson, and M. B. Denton, *Appl. Spectrosc.* **41**, 1114 (1987).
5. R. B. Bilhorn, P. M. Epperson, J. V. Sweedler, and M. B. Denton, *Appl. Spectrosc.* **41**, 1125 (1987).
6. J. V. Sweedler, R. D. Jalkian, and M. B. Denton, *Appl. Spectrosc.* **43**, 953 (1989).
7. D. K. Schroder in "Advanced MOS Devices", Volume VI of "Series on Solid State Devices", G. W. Neudeck and R. F. Pierret, Eds. (Addison-Wesley, Reading, 1987), Ch. 3-4.
8. J. Janesick and M. Blouke, *Sky and Telescope*. September, (1987).
9. Photometrics Ltd., Series 200 CCD Camera System User's Manual Version 6.0. (Photometrics Ltd., Tucson, Arizona, January 1989).
10. M. M. Blouke, D. L. Heidtmann, B. Corrie, M. L. Lust, and J. R. Janesick in "Solid State Imaging Arrays", K. N. Prettyjohns and E. L. Dereniak, Eds. (1985), p. 82.
11. G. Beal, G. Boucharlat, J. Chabbal, J-P. Dupin, B. P. Fort, and Y. Mellier, *Opt. Eng.* **26**, 902 (1987).
12. J. E. Pemberton, R. L. Sobocinski, and G. Sims, *Appl. Spectrosc.* **44**, 328 (1990).
13. J. Muskovic, Princeton Instruments (private communication).

14. B. P. Straughan in "Spectroscopy, Vol. 2", B. P. Straughan and S. Walker, Eds. (Hallstead Press: New York, 1976), pp. 257-258.



## FIGURE CAPTIONS

1. The serial (A-D) and parallel (E-H) binning geometries of the TH 7882 CCD.  
Serial-binning Geometry: (A) The CCD is exposed to light and an pattern of charge accumulates on the parallel register; (B) Charge from the first of the 576 "rows" is shifted into the serial register while charge on the remaining 575 "rows" is shifted one "row" towards the serial register; (C) Charge in the serial register is binned (summed) into the output node where it is amplified and digitized; (D) The serial register is now clear and the next "row" of charge is shifted into the serial register.  
Parallel-binning Geometry: (E) The CCD is exposed to light and an pattern of charge accumulates on the parallel register; (F-G) The charge image on the CCD is binned (summed) into the serial register; (H) Each of the 374 "columns" of charge is individually shifted into the output node for digitization.
2. The  $214\text{ cm}^{-1}$  band of carbon tetrachloride (baseline subtracted) taken at integration times of 5, 30, and 100 seconds. The spectra acquired at the two shorter exposures were scaled so that the band widths could be compared. The spectral axis, proportional to wavelength, is plotted in units of the CCD pixel spacing since the charge-trapping artifact is a characteristic of the detector. (a) CCD oriented in the serial-binning geometry with no preflash. (b) CCD oriented in a parallel-binning geometry with no preflash.
3. Width of carbon tetrachloride  $214\text{ cm}^{-1}$  band in pixels as a function of integration time, for the CCD oriented in the serial-binning geometry.

4. Width of carbon tetrachloride  $214\text{ cm}^{-1}$  band in pixels as a function of integration time for the CCD oriented in the parallel-binning geometry.
5. Center position for the carbon tetrachloride  $214\text{ cm}^{-1}$  band in pixels as a function of integration time, for the CCD oriented in the serial-binning geometry.
6. Width of carbon tetrachloride  $214\text{ cm}^{-1}$  band in pixels as a function of integration time for the CCD oriented in the serial-binning geometry; the response at two detector temperatures is plotted.
7. Log of detector sensitivity (slope of intensity versus integration time) versus inverse of the detector temperature. Parallel-binning geometry shows no significant  $T$  dependence, while a loss of sensitivity in the serial-binning geometry at higher temperatures follows Arrhenius behavior.

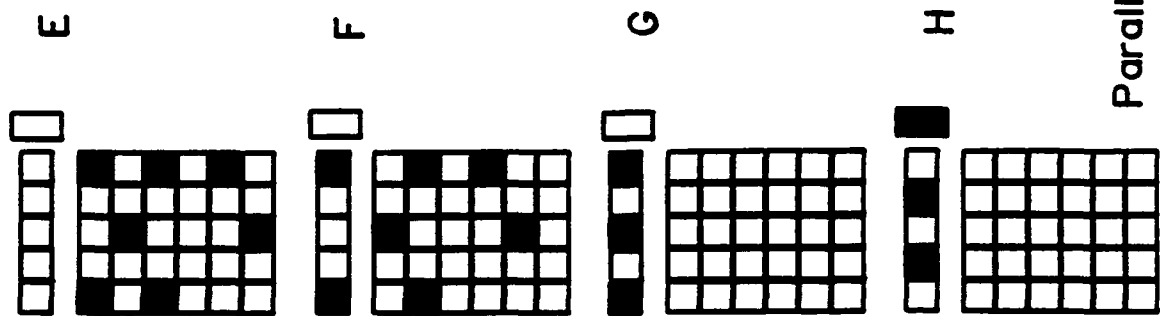
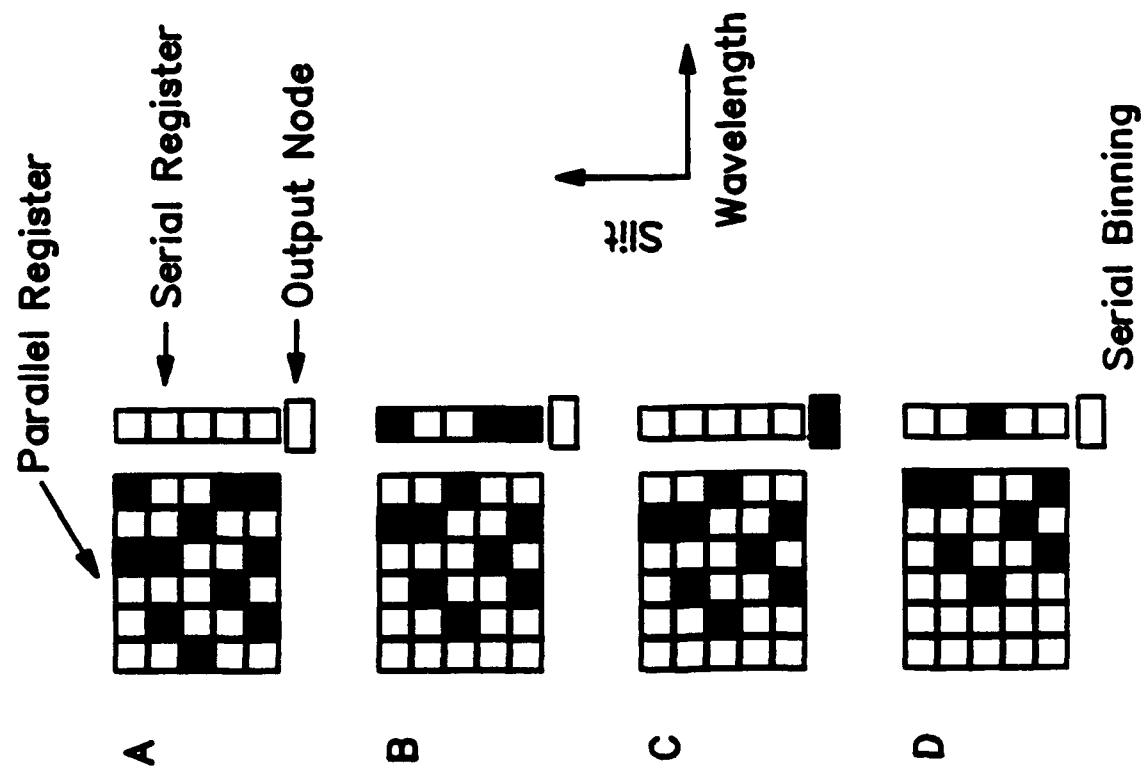


Figure 1

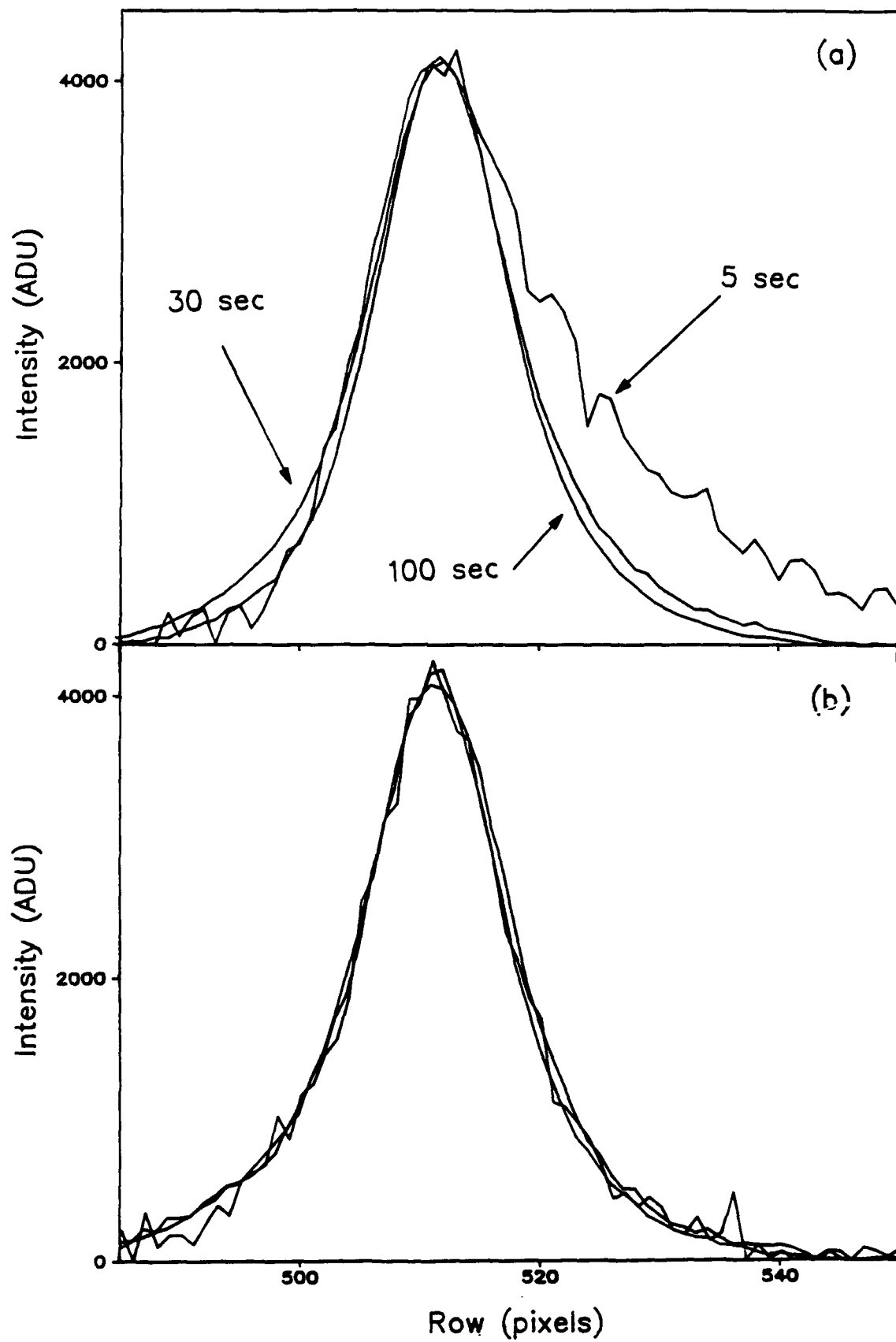


Figure 2a  
2b

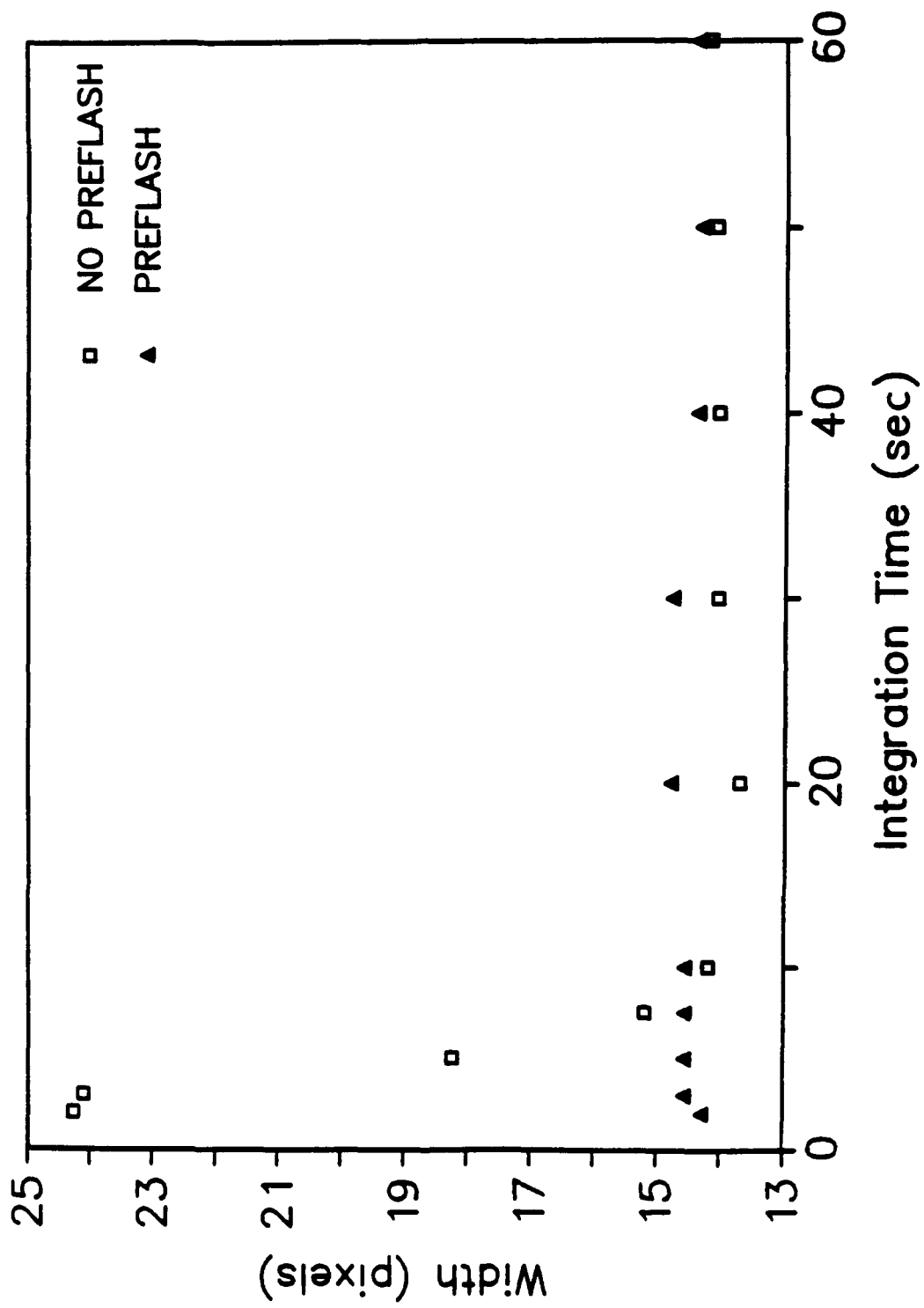


Figure 3

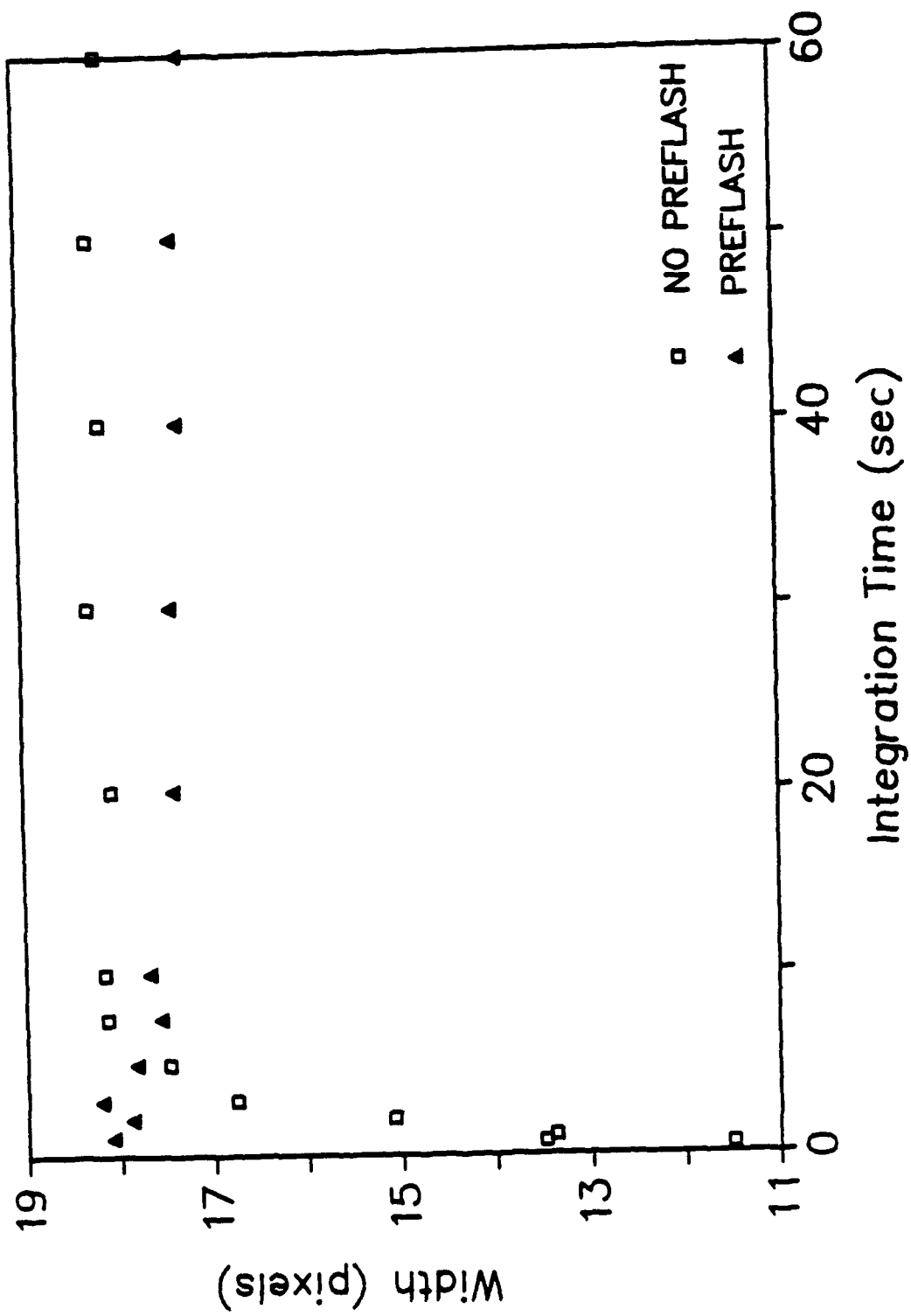


Figure 4

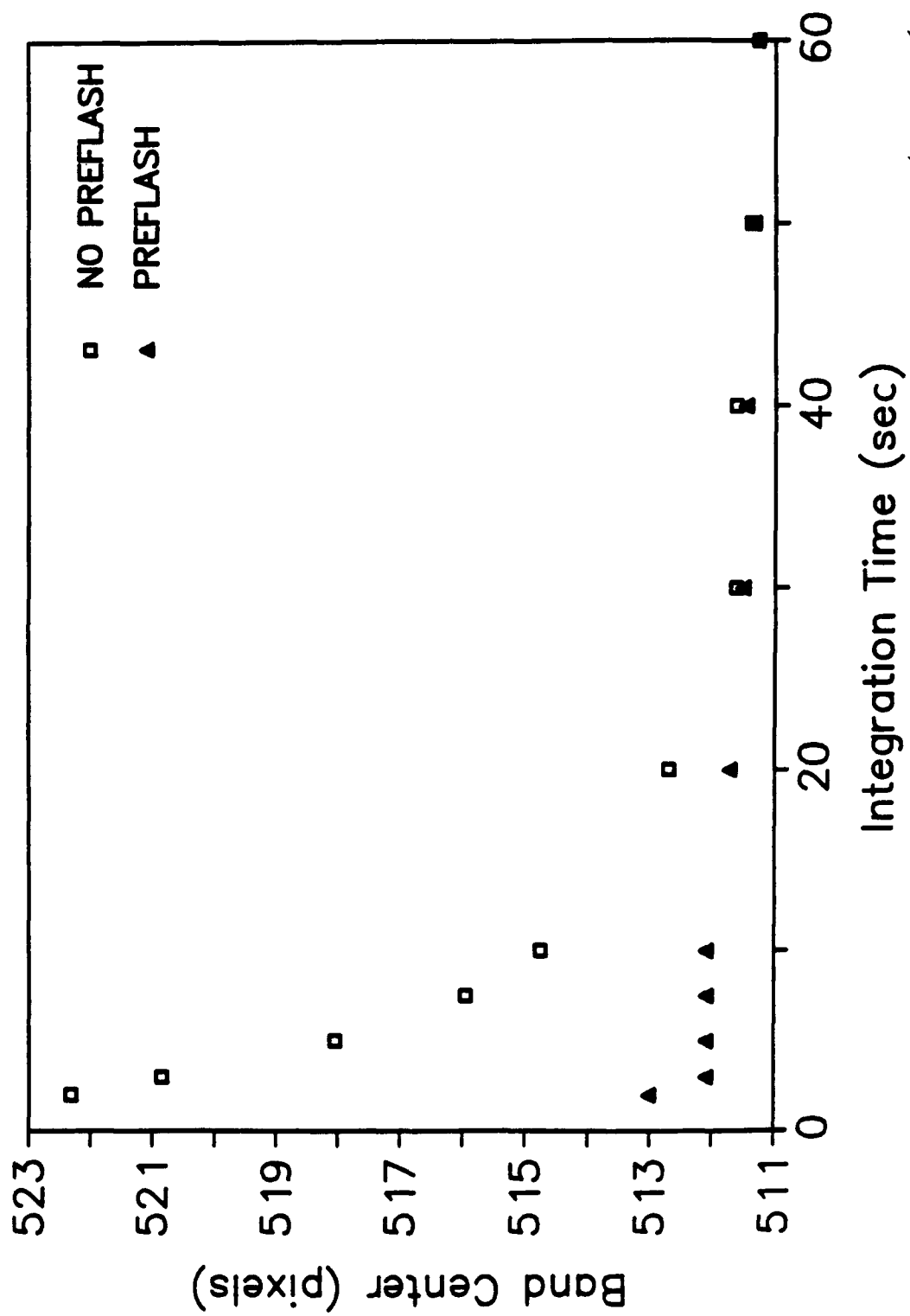


Figure 5

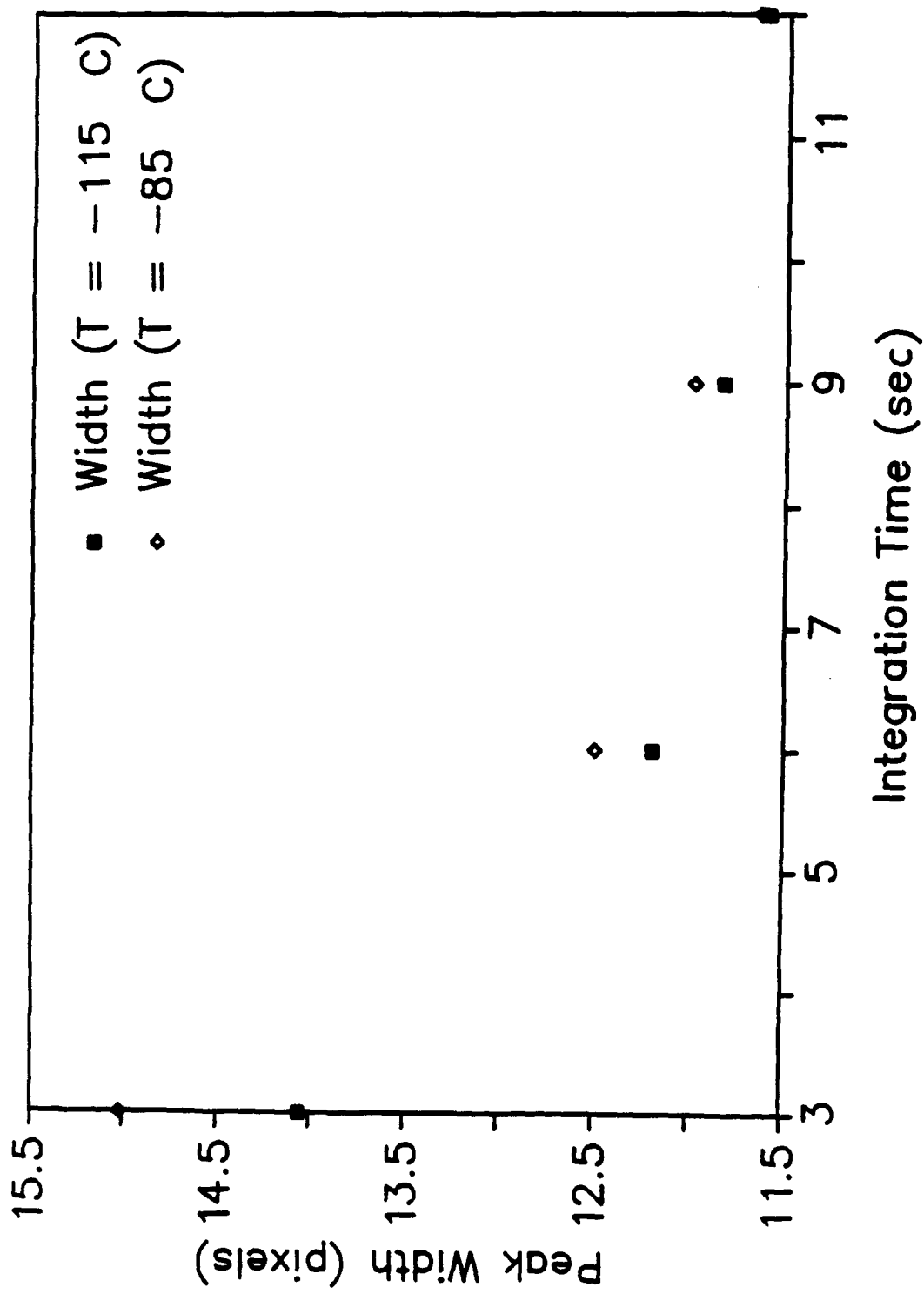


Figure 6



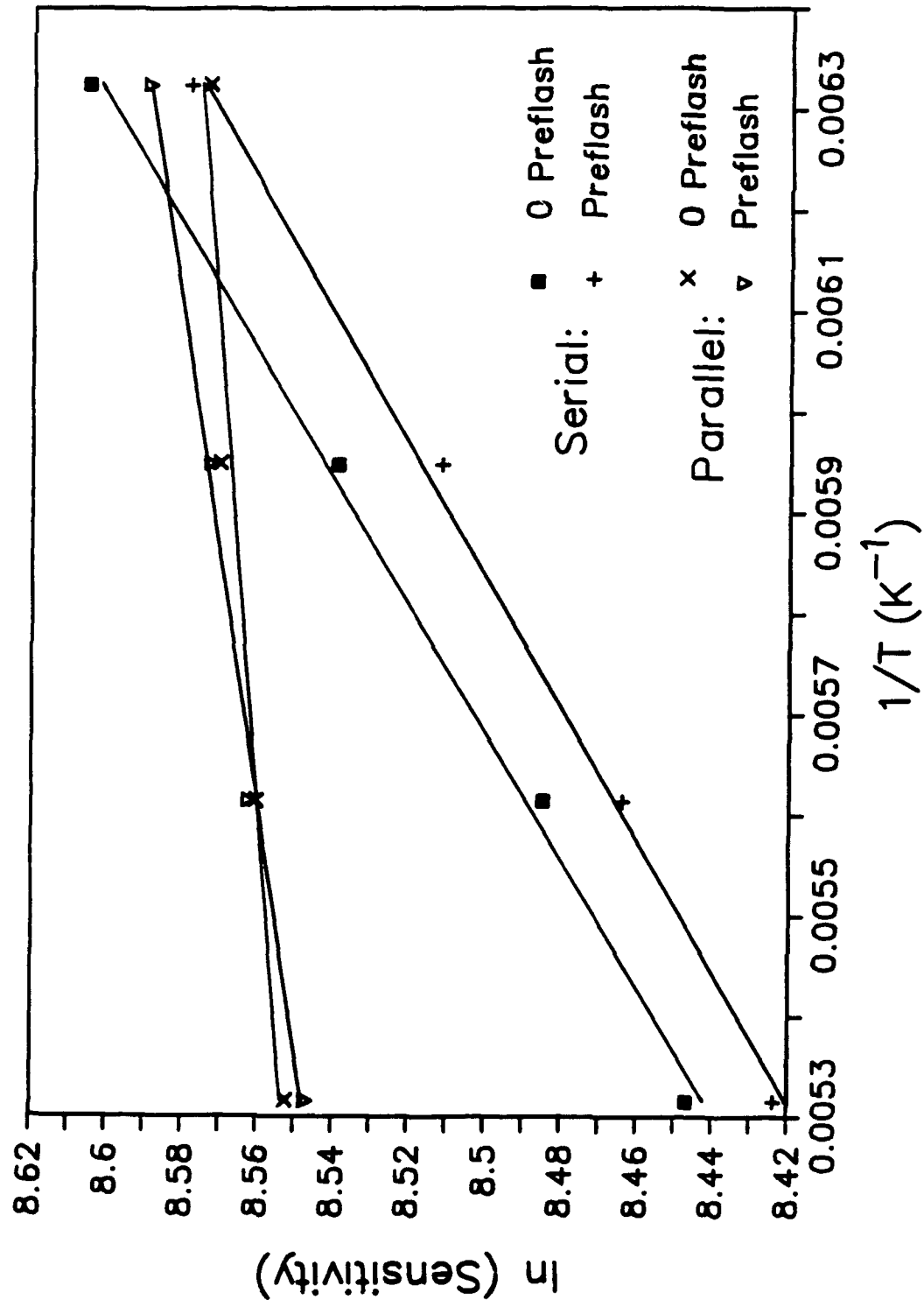


Figure 7